

# Large Sagnac frequency splitting in a ring resonator operating at an exceptional point

Satoshi Sunada

*Faculty of Mechanical Engineering, Institute of Science and Engineering, Kanazawa University,  
Kakuma-machi Kanazawa, Ishikawa 920-1192, Japan*

(Received 28 April 2017; revised manuscript received 1 September 2017; published 25 September 2017)

In rotating ring resonators, resonant frequencies are split because of the Sagnac effect. The rotation sensitivity of the frequency splitting characterizes the sensitivity of resonator-based optical gyroscopes. In this paper, it is shown that the sensitivity of frequency splitting can be significantly enhanced in a ring resonator operating at an exceptional point (EP), which is a non-Hermitian degeneracy where two eigenvalues and the corresponding eigenmodes coalesce. As an example, a ring resonator with a periodic structure is proposed and theoretically and numerically studied. It is numerically demonstrated that in the resonator operating near an EP, the rotation-induced frequency splitting can be more than two orders greater than that in conventional ring resonators. In addition, this paper discusses the influence of the resonator loss on the measurement sensitivity of the frequency splitting and a method of rotation detection based on rotation-induced changes of eigenmodes near an EP.

DOI: [10.1103/PhysRevA.96.033842](https://doi.org/10.1103/PhysRevA.96.033842)

## I. INTRODUCTION

Optical gyroscopes are highly sensitive rotation sensors [1–3]. They are widely used as key components of inertial navigation systems in many industrial and military applications, such as airplanes, ships, satellites, and so on. Considerable research effort has been devoted to realizing chip-scale compact optical gyroscopes [4–17] because such small and navigation-grade rotation sensors have the potential to be used in mobile platforms and may extend into numerous applications. However, the sensitivity of an optical gyroscope decreases as the size of the sensing element decreases. This is because the operating principle is based on the Sagnac effect [18], which manifests itself in the form of a phase shift in a rotating ring interferometer and frequency splitting between clockwise (CW) and counterclockwise (CCW) propagating modes in a rotating ring resonator. The splitting is referred to as Sagnac frequency splitting (SFS). The rotation sensitivity of SFS is proportional to the effective size of the resonator, which is obtained by dividing the enclosed area by the perimeter of the closed optical path in the resonator [1].

Thus far, many proposals for enhancing the sensitivity of SFS have been made [17,19–24]. Most of them are based on enhancement using the effect of anomalous dispersion [19–24]. The SFS can be made larger by the effect of anomalous dispersion of superluminal light propagation in a resonator [19]. Although the enhancement using anomalous dispersion seems to be promising, it has been pointed out that strong dispersion systems are essentially accompanied by intense loss or significant linewidth broadening [25,26].

Meanwhile, a general theory on the sensitivity enhancement of sensors using resonators has been recently presented in the context of non-Hermitian physics in microcavities [27], and several applications have been proposed [28–31]. The basic idea of the enhancement is to use an anomalous perturbation response at the so-called exceptional point (EP) in non-Hermitian resonator systems. An EP is a non-Hermitian degeneracy, where two or more eigenvalues and the corresponding eigenmodes coalesce [32–34], and it is distinct from Hermitian degeneracy (normal degeneracy), where the eigenmodes of the degenerate eigenvalues are linearly independent. The occurrences of EPs have been experimentally and numerically

demonstrated in a variety of systems [35–42]. If the system with two coalescing eigenvalues at an EP is subjected to a perturbation of strength  $\epsilon$ , the magnitude of the resulting eigenvalue splitting is typically proportional to  $\epsilon^{1/2}$  [27,32,43–46]. For weak perturbation of strength  $\epsilon \ll 1$ , the  $\epsilon^{1/2}$ -order splitting is much greater than the  $\epsilon$ -order splitting of normal degenerate eigenmodes.

In this paper, the enhancement of the sensitivity of SFS by using EPs is studied. A ring resonator that can operate at an EP is considered and the SFS arising in the resonator is analyzed. It is theoretically and numerically shown that the SFS in the resonator is significantly greater than that in conventional ring resonators. In addition, this paper discusses the influence of resonator loss on the measurement sensitivity of SFS and a rotation detection method using the rotation-induced changes of the eigenmodes near an EP.

## II. PERTURBATION SENSITIVITY AT EP

This section briefly introduces a perturbation theory for non-Hermitian matrix operators [43,44], and we discuss the condition for enhancing the sensitivity to rotation perturbation. Non-Hermiticity is a requirement for the existence of an EP and can be introduced by loss or gain in resonator systems. In this study, we consider a resonator system that is described by a non-Hermitian effective Hamiltonian matrix  $\hat{H}_0$ . It is assumed that the system is at an EP, where only two eigenvalues and the corresponding eigenvectors of  $\hat{H}_0$  coalesce. Let us denote the coalescing eigenvalue as  $E_0$  and right or left eigenvectors as  $\mathbf{u}_0$  or  $\mathbf{v}_0$  at an EP, satisfying  $\hat{H}_0\mathbf{u}_0 = E_0\mathbf{u}_0$  and  $\mathbf{v}_0^\dagger\hat{H}_0 = E_0\mathbf{v}_0^\dagger$  [44,47], where  $\dagger$  denotes Hermitian conjugate.

Once the system at the EP is subject to perturbation of  $\epsilon$  order, so that the matrix operator is changed to  $\hat{H} = \hat{H}_0 + \epsilon\hat{H}_1$ , where  $\hat{H}_1$  is a perturbation, the eigenvalues of the perturbed system split into two as follows:

$$E_{\pm} = E_0 \pm \epsilon^{1/2} \sqrt{\mathbf{v}_0^\dagger \hat{H}_1 \mathbf{u}_0} + O(\epsilon), \quad (1)$$

and the corresponding right eigenvectors also split into two,

$$\mathbf{u}_{\pm} = \mathbf{u}_0 + (E_{\pm} - E_0)\mathbf{u}_1 + O(\epsilon), \quad (2)$$

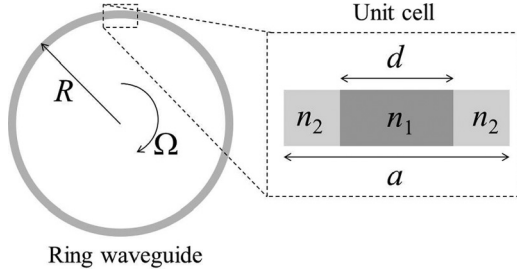


FIG. 1. Ring resonator consisting of  $N$  unit cells of arc length  $a$ .  $n_1$  and  $n_2$  are complex-valued refractive indices in a unit cell.  $R$  is the ring radius. The ring waveguide is a one-dimensional waveguide.

where  $\mathbf{u}_1$  is the associate vector defined by  $(\hat{H}_0 - E_0)\mathbf{u}_1 = \mathbf{u}_0$  and the normalization condition  $\mathbf{v}_0^\dagger \cdot \mathbf{u}_1 = 1$  [43]. It is important to note that the square-root response to perturbation does not always occur at an EP; however, it depends on the eigenvectors and perturbation types. Indeed, the condition for the square-root response is

$$\mathbf{v}_0^\dagger \hat{H}_1 \mathbf{u}_0 \neq 0. \quad (3)$$

If  $\mathbf{u}_0$  is also the right eigenvector of perturbation  $\hat{H}_1$ ,  $\mathbf{v}_0^\dagger \hat{H}_1 \mathbf{u}_0 = E_1 \mathbf{v}_0^\dagger \cdot \mathbf{u}_0$  is derived, where  $E_1$  is the eigenvalue of  $\hat{H}_1$ , and the inner product  $\mathbf{v}_0^\dagger \cdot \mathbf{u}_0$  is zero at the EP because of the self-orthogonality [43]. In this case, condition (3) is not satisfied, and the eigenvalue splitting becomes smaller than the order of  $\epsilon^{1/2}$ .

Here, let us consider the condition for enhancing rotation sensitivity by applying the above results to ring resonators. Rotation is regarded as a perturbation to the resonator. As shown in the next section, rotation perturbation can be described by a momentum operator  $i\partial/\partial x$  [see Eq. (4)], the eigenmodes of which are CW and CCW modes,  $e^{\pm ikx}$ , where  $k$  is an eigenvalue of the operator. Therefore, resonators with CW or CCW mode as an eigenmode do not satisfy condition (3) even if the resonator operates at an EP. The example can be seen in a microcavity with asymmetric backscattering [48].

### III. RING RESONATOR OPERATING AT EP

One of ring resonators satisfying condition (3) is a coupled ring resonator with parity-time symmetry [31]. However, the resonator structure leads to rotation dependence of the eigenmode loss (or amplification), which may affect the sensitivity of rotation detection. This section proposes another type of ring resonator, which satisfies condition (3) without such rotation dependence. The ring resonator has a one-dimensional periodic structure along the ring waveguide, which consists of  $N$  unit cells of arc length  $a$ . Suppose the ring radius is  $R$ , and the length of the waveguide is  $L (= Na = 2\pi R)$ . It is assumed that the waveguide is a single-mode waveguide and the radius  $R$  is much larger than the width of the waveguide. Figure 1 illustrates an example of a ring resonator with a periodic structure, where the unit cells are characterized by two refractive indices  $n_1$  and  $n_2$ . A periodic structure generally induces coupling between CW and CCW modes in the ring resonator. Therefore, the eigenmodes of the resonator are not pure CW or CCW modes [49,50]. The resonator can be made

to operate at an EP by engineering absorption or radiation losses.

We consider the case when the ring resonator is rotating clockwise with angular velocity  $\Omega$  in a plane and that the electric field is perpendicular to the plane and oscillates as  $\Psi e^{-i\omega t}$  in the rotating resonator, where  $\omega$  is an angular frequency. The field  $\Psi$  satisfies the following wave equation [50–52],

$$\left[ \frac{\partial^2}{\partial x^2} + n^2 \left( \frac{\omega}{c} \right)^2 + 2i \left( \frac{\omega}{c} \right) \Omega_D \frac{\partial}{\partial x} \right] \Psi = 0, \quad (4)$$

where  $x$  denotes a coordinate along the ring waveguide in the rotating frame of reference. It is assumed that the field  $\Psi$  can be characterized only by  $x$  dependence because of the one-dimensional ring structure.  $\Omega_D = R\Omega/c$  is the dimensionless angular velocity, and  $c$  is the speed of light in vacuum.  $n(x)$  is a complex-valued refractive index and it is periodic with period  $a$  so that  $n(x+a) = n(x)$ . The imaginary part  $\text{Im} n(x)$  characterizes the loss in the resonator, so that the resonator system is non-Hermitian.  $\Psi(x)$  and  $\omega$  obtained by solving Eq. (4) under the periodic boundary condition  $\Psi(x) = \Psi(x+L)$  are an eigenmode and eigenfrequency of the ring resonator, respectively. Because of the non-Hermiticity of the resonator,  $\omega$  is a complex-valued frequency. The real part is the resonant frequency of the eigenmode, and the imaginary part denotes the decay rate of the mode, which characterizes the spectral linewidth at the resonance.

According to the Bloch(-Floquet) theorem, the field in a periodic medium takes the form  $\Psi = \psi_\kappa(x)e^{i\kappa x}$ , where  $\kappa$  is the Bloch wave number and  $\psi_\kappa(x)$  is a periodic function with period  $a$  so that  $\psi_\kappa(x+a) = \psi_\kappa(x)$ . Because of the periodic boundary condition of the resonator, the Bloch wave number is discretized as  $\kappa = 2\pi l/L$  [53], where  $l$  is an integer.

In systems with periodic structures, such as photonic crystals, there are EPs near a  $\Gamma$  point ( $\kappa = 0$ ) of the Bloch wave-number space [37,54]. For  $\kappa a \ll 1$  and  $|\Omega_D| \ll 1$ , the eigenmode is determined by the wave equation

$$\left[ \frac{\partial^2}{\partial x^2} + n^2 \left( \frac{\omega}{c} \right)^2 + 2i \left( \kappa + \frac{\omega}{c} \Omega_D \right) \frac{\partial}{\partial x} \right] \psi_\kappa = 0, \quad (5)$$

where  $-a/2 \leq x < a/2$  and the second orders of  $\kappa a$  and  $\Omega_D$  are omitted.

We focus on a resonator where the unit cell is symmetric with respect to  $x = 0$  so that  $n(-x) = n(x)$ . When  $\Omega = 0$ , there are nearly degenerate eigenmodes at  $\kappa = 0$ , the wave functions of which are even and odd functions with respect to  $x = 0$ . We label the nearly degenerate modes as  $j = 1, 2$ . The wave function  $\phi_j$  of eigenmode  $j$  is described by  $[\frac{\partial^2}{\partial x^2} + n^2(\frac{\omega_j}{c})^2]\phi_j = 0$ , where  $\omega_j$  is the eigenfrequency of the mode  $j$ .  $\phi_1$  and  $\phi_2$  can satisfy the following relations:

$$\int_{-a/2}^{a/2} \phi_i \phi_j n^2 dx = \delta_{ij}, \quad (6)$$

$$\int_{-a/2}^{a/2} \phi_i \frac{\partial \phi_j}{\partial x} dx = - \int_{-a/2}^{a/2} \phi_j \frac{\partial \phi_i}{\partial x} dx. \quad (7)$$

For  $\kappa \neq 0$  and  $\Omega_D \neq 0$ , we describe the wave function  $\psi_\kappa$  as  $c_1 \phi_1 + c_2 \phi_2$  and substitute it into Eq. (5). After some

calculations with Eqs. (6) and (7), we have

$$(\hat{H}_0 + \epsilon \hat{H}_1)\mathbf{u} = \omega \mathbf{u}, \quad (8)$$

where

$$\hat{H}_0 = \begin{pmatrix} \omega_0 - \frac{\Delta\omega_0}{2} & -i \frac{\alpha_0 c \kappa}{\omega_0} \\ i \frac{\alpha_0 c \kappa}{\omega_0} & \omega_0 + \frac{\Delta\omega_0}{2} \end{pmatrix}, \quad \hat{H}_1 = \begin{pmatrix} 0 & -i \\ i & 0 \end{pmatrix}, \quad (9)$$

and  ${}^t\mathbf{u} = (c_1, c_2)$ . In the above,  $\epsilon = \alpha_0 \Omega_D$ ,  $\Delta\omega_0 = \omega_2 - \omega_1$ ,  $\omega_0 = (\omega_1 + \omega_2)/2$ , and  $\alpha_0 = c \int \phi_1 \frac{\partial \phi_2}{\partial x} dx$ .

When  $\Omega_D = 0$ , the eigenvalues of the effective Hamiltonian  $\hat{H}_0$  are  $\omega = \omega_0 \pm \Delta\omega_0/(2\beta_0)\sqrt{\beta_0^2 + 1}$ , where  $\beta_0 = \omega_0 \Delta\omega_0/(2\alpha_0 c \kappa)$ . When  $\beta_0^2 = -1$ , the two eigenvalues and corresponding eigenvectors coalesce.

When  $\Omega_D > 0$ , the coalescing eigenfrequencies and eigenvectors at the EP split into two due to the rotation perturbation  $\hat{H}_1$ . According to Eq. (1), the splitting frequencies are described as follows:

$$\omega_{\pm} = \omega_0 \pm \sqrt{\frac{2\alpha_0^2 c \kappa}{\omega_0} \Omega_D + O(|\alpha_0 \Omega_D|)}, \quad (10)$$

and the corresponding right eigenvectors are

$$\mathbf{u}_{\pm} \approx \mathbf{u}_0 + (\omega_{\pm} - \omega_0)\mathbf{u}_1, \quad (11)$$

where  ${}^t\mathbf{u}_0 = (1, i\beta_0)$  and  ${}^t\mathbf{u}_1 = -\frac{1}{\Delta\omega_0}(1, -i\beta_0)$ .

When the modes at the EP are such low-loss modes that  $|\text{Im} \omega_0| \ll \text{Re} \omega_0$  and the spatial variation of  $n$  is sufficiently small,  $\alpha_0$  is approximated by  $\text{Re} \omega_0/n_0$ , where  $n_0$  is the spatially averaged refractive index. In this case, the magnitude of SFS at the EP can be expressed as  $\Delta\omega_{EP} = |\text{Re}(\omega_{\pm} - \omega_0)| \approx \sqrt{|\text{Im} \Delta\omega_0| \text{Re} \omega_0 \Omega_D/n_0}$ . Meanwhile, in conventional ring resonators without any periodic structures but with the same index and same radius, the magnitude of SFS is given by  $\Delta\omega_{NS} = (\text{Re} \omega_0/n_0)\Omega_D$  [19,52]. The enhancement factor  $\eta$  defined by the ratio of  $\Delta\omega_{EP}$  to  $\Delta\omega_{NS}$  is

$$\eta = \frac{\Delta\omega_{EP}}{\Delta\omega_{NS}} \approx \sqrt{\frac{|\text{Im} \Delta\omega_0| n_0}{\text{Re} \omega_0 \Omega_D}}. \quad (12)$$

The SFS can be enhanced in the range  $0 < \Omega_D < |\text{Im} \Delta\omega_0| n_0 / \text{Re} \omega_0$ .

#### IV. NUMERICAL DEMONSTRATION

In this section, the enhancement of the SFS near an EP is numerically demonstrated in the ring resonator shown in Fig. 1, which consists of two materials with refractive indices  $n_1$  and  $n_2$ . The following parameters were used for this demonstration:  $n_1^2 = 13.095$ ,  $n_2^2 = 13.10 + i0.055$ , and  $d = 0.49455a$ . Figure 2 shows eigenfrequency  $\omega$  as a function of  $\kappa$ , which represents a band curve defined in the limit  $N \rightarrow \infty$ . When  $\Omega_D = 0$ , two eigenfrequencies almost coalesce at  $\kappa = \kappa_{EP} \approx 1.1638 \times 10^{-5} (2\pi/a)$ .

The enhancement of the SFS arising near the EP can be visually understood based on the shift of the band curve in the presence of rotation. When  $\Omega_D > 0$ , the band curve is shifted in the direction of  $\kappa < 0$ , so that resonant frequencies  $\text{Re} \omega$  change for each  $\kappa$  value [Fig. 2(a)]. The largest shifts of resonant frequencies arise for the eigenmodes at  $\kappa = \kappa_{EP}$ ,

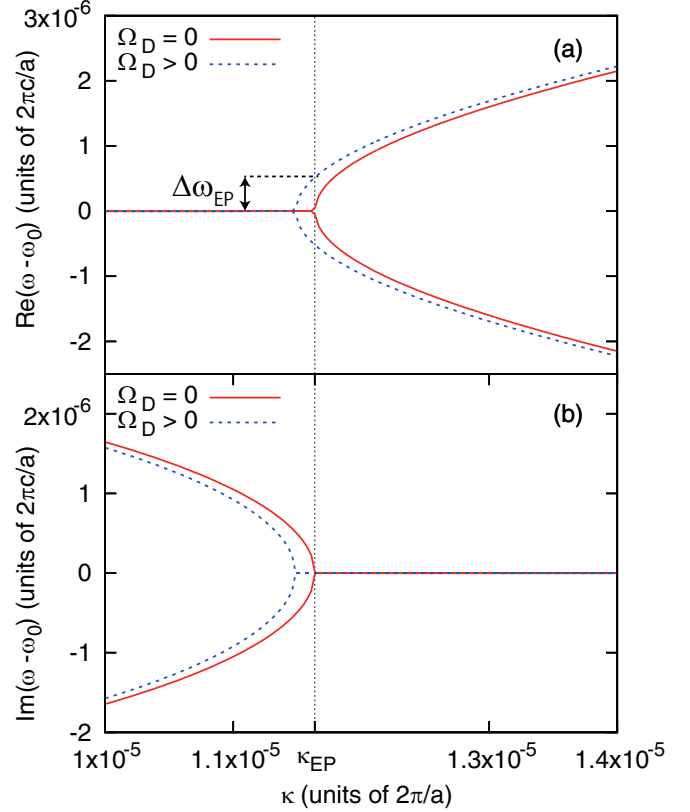


FIG. 2. Eigenfrequency  $\omega$  as a function of Bloch wave number  $\kappa$ , which corresponds to a complex band curve defined in the limit  $N \rightarrow \infty$ . (a) Real and (b) imaginary parts of frequency  $\omega$  are shown as a function of  $\kappa$ .  $\omega_0$  is an eigenfrequency coalescing at the EP when  $\Omega_D = 0$ . When  $\Omega_D > 0$ , the band curve is shifted and resonant frequencies change for each eigenmode at a given  $\kappa$  value. The largest frequency shifts arise at  $\kappa = \kappa_{EP}$ , whereas the decay rates almost do not change.

whereas the decay rates of the modes almost do not change [Fig. 2(b)].

In order to ensure that  $\kappa$  approaches  $\kappa_{EP}$  in an actual experiment, the number of cells  $N$  should be as large as possible because of  $\kappa = 2\pi l/(Na)$ . In the simulation, we set  $l = 1$ ,  $N = 85925$ , i.e.,  $\kappa a/(2\pi) = 1.163806 \times 10^{-5}$ . (For this  $N$  value, the radius  $R = Na/(2\pi)$  will be 3.8 mm if the optical wavelength  $2\pi c/\text{Re} \omega_0$  and  $a$  are 1  $\mu\text{m}$  and 0.276  $\mu\text{m}$ , respectively.) Figure 3(a) shows the rotation dependences of the resonant frequencies and decay rates of eigenmodes at the  $\kappa$  value. Figure 3(b) shows the enhancement factor  $\eta$  as a function of  $\Omega_D$ . More than 100 times enhancement can be achieved for  $\Omega_D < 5 \times 10^{-9}$ , which corresponds to  $2.3 \times 10^4$  deg/s in a ring resonator of radius  $R = 3.8$  mm.

#### V. DISCUSSION

##### A. Effects of resonator loss and gain

According to Eq. (12), the enhancement factor  $\eta$  can be increased by increasing  $|\text{Im} \Delta\omega_0|$ ; however, it is limited by the average decay rate  $|\text{Im} \omega_0|$  when the resonator is a passive system. This means that large resonator losses are needed for

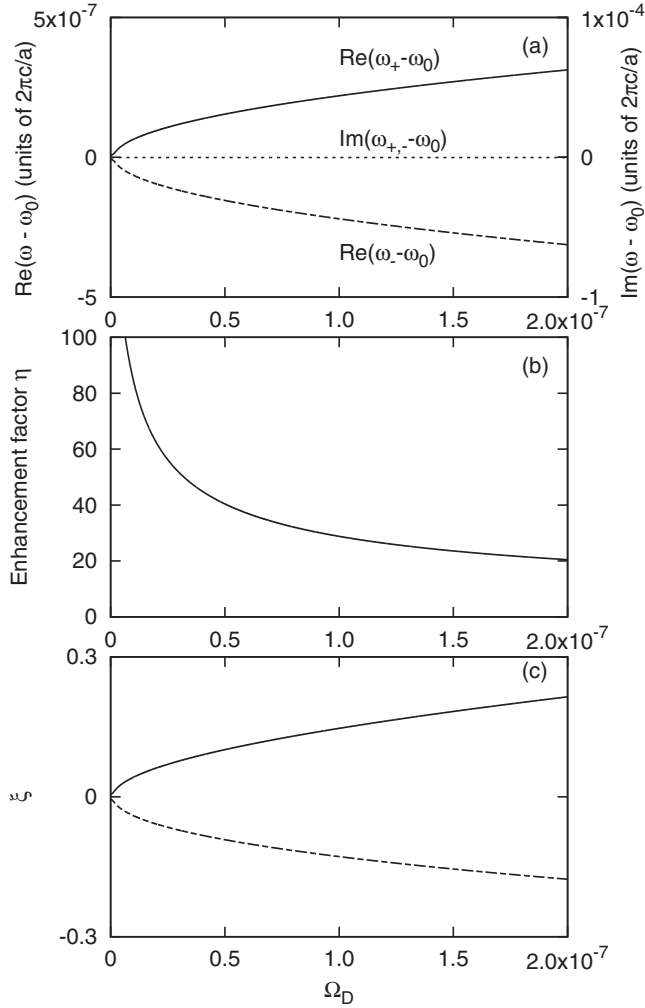


FIG. 3. (a) Real and imaginary parts of eigenfrequency shifts  $\omega_{\pm} - \omega_0$  at  $\kappa \approx \kappa_{EP}$  as a function of  $\Omega_D$ . (b) Enhancement factor  $\eta = \Delta\omega_{EP}/\Delta\omega_{NS}$  as a function of  $\Omega_D$ . (c)  $\xi$  of the eigenmodes with frequency  $\omega_+$  (solid curve) and  $\omega_-$  (dashed curve) at  $\kappa \approx \kappa_{EP}$  [see Eq. (13)].

enhancing the SFS, resulting in spectral linewidth broadening and the decrease in the sensitivity of rotation detection [55].

A way to solve the tradeoff between the enhancement of SFS and loss reduction is to include optical gain in resonators [27]. If the gain is introduced in a resonator, the resonator losses can be reduced, while  $|\text{Im} \Delta\omega_0|$  and thus enhancement factor  $\eta$  are maintained. This can be analytically shown when the variation of refractive index  $n$  is small so that  $\int \phi_1^2 dx \approx \int \phi_2^2 dx \approx 1/n_0^2$  and  $|\text{Re} n| \gg |\text{Im} n|$ . The effect of the gain is incorporated in Eq. (4) by changing the imaginary part of the refractive index  $\text{Im} n^2$  to  $\text{Im} n^2 - g$ , where  $g > 0$  is a gain coefficient. We obtain the eigenfrequency  $\omega_{\pm} \approx \omega_0 + ig\omega_0/(2n_0^2) \pm \Delta\omega_{EP}$ . The magnitude of SFS is not changed by the gain, whereas the decay rate  $|\text{Im} \omega_{\pm}|$  decreases as  $g$  increases.

In general, when gain exceeds loss and lasing occurs, nonlinear coupling, e.g., lock-in phenomenon, occurs among modes [1], which may make it difficult to operate at an EP. To avoid nonlinear mode coupling phenomena, gain should

not exceed the lasing threshold value. SFS can be measured by detecting the shifts of the resonant frequencies, such as resonant gyroscopes [55].

### B. Rotation-induced changes of eigenmodes and alternative rotation sensing approach

According to Eq. (11), the right eigenvector  ${}^t\mathbf{u} = (c_1, c_2)$  at an EP strongly depends on rotation, which means that the wave function  $\psi_{\kappa} = c_1\phi_1 + c_2\phi_2$  is changed by rotation. The rotation dependence of the wave function is a unique characteristic of the ring resonator operating at an EP, and it can be exploited as an alternative rotation sensing approach [8]. In this approach, rotation can be measured without a direct dependence on the spectral linewidth of the resonator.

Here, we measure changes in the wave functions of eigenmodes by using the ratio of the CCW wave components to the CW wave components,

$$\xi = \frac{\sum_{m>0} |a_m|^2}{\sum_{m<0} |a_m|^2} - 1, \quad (13)$$

where  $a_m = \int \psi_{\kappa} e^{-ik_m x} dx$  is the Fourier transform of  $\psi_{\kappa}$  to the wave number domain,  $k_m = 2\pi m/a$  ( $m$  is an integer).  $a_m$  denotes a CCW (CW) wave component with angular momentum  $m$  when  $m$  is positive (negative).  $\xi$  can be measured experimentally by coupling a waveguide to the ring resonator and monitoring the changes in the coupling intensities of CW and CCW waves.

Figure 3(c) shows  $\xi$  obtained for each eigenmode at  $\kappa \approx \kappa_{EP}$ . When  $\Omega_D = 0$ , the CW and CCW wave components are balanced (i.e.,  $\xi = 0$ ), which means that the eigenmodes are standing waves. As  $\Omega_D$  increases, the eigenmode corresponding to frequency  $\omega_{+(-)}$  has a larger CCW (CW) wave component.  $\xi$  changes greatly at low rotation rates because of the square-root behavior. If  $\xi = 10^{-4}$  is experimentally detectable in the resonator operating just at the EP, the minimum detectable rotation rate is approximately  $4.5 \times 10^{-14}$ , which corresponds to 0.2 deg/s for the resonator with  $R = 3.8$  mm. As  $R$  increases, the minimum detectable rotation rate can be further reduced.

### C. Two technical difficulties for sensing applications

Lastly, we comment on two technical difficulties of rotation detection by using ring resonators operating at an EP. The first one is rotation detection for  $\Omega_D < 0$ . As seen in Eq. (10), when  $\Omega_D < 0$ , the resonant frequencies at  $\kappa = \kappa_{EP} > 0$  almost do not change but the decay rates split into two. Consequently, inverse rotation  $\Omega_D < 0$  cannot be measured from the SFS. However, even when  $\Omega_D < 0$ , the SFS arises at  $\kappa = -\kappa_{EP}$  because of the symmetry of Eq. (4). At least two ring resonators operating at  $\kappa = \pm\kappa_{EP}$  would be needed for practical rotation sensing.

The second difficulty stems from fabrication imperfections or parameter mismatches, which induce unwanted frequency shifts and degrade the sensitivity to rotation. For instance, when the resonator has a periodic structure but the refractive index  $n$  is perturbed as  $n + \Delta n(x)$  and there is a deviation from the condition  $\beta_0^2 = -1$ , the resulting frequency difference  $(\omega_+ - \omega_-)/2$  between the two modes can be estimated as

$\sqrt{\delta + \eta}$ , where  $\delta = \Delta\omega_0^2/4 + (c\kappa/\omega_0 + \Omega_D)^2\alpha_0^2$  and  $\eta$  is a function of  $\Delta n_{ij}^2 = \int \phi_i \Delta n^2 \phi_j dx$ . Therefore, an approach that precisely accesses EPs would be needed, such as an active tuning of device geometry or parameters by using two fiber tips [56,57].

## VI. SUMMARY

This paper showed a condition for enhancing SFS by using EPs and proposed a ring resonator with a periodic structure that satisfies the condition. It was shown that the SFS of the eigenmodes near an EP can be greatly enhanced compared to that of conventional ring resonators at low rotation rates.

The resonator loss can be reduced by optical gain without affecting the enhancement factor of the SFS. In addition, it was also shown that the ring resonator operating at an EP has the unique feature that the wave functions of the eigenmodes are drastically changed by rotation. The changes in the wave functions can be used as an alternative approach to rotation detection without a direct dependence on the spectral linewidth of the resonator.

## ACKNOWLEDGMENTS

S.S. thanks Prof. T. Harayama, Dr. S. Shinohara, and Dr. T. Niiyama for their comments and discussions. This work was partially supported by JSPS KAKENHI Grant No. 16K04974.

- 
- [1] W. W. Chow, J. Gea-Banacloche, L. M. Pedrotti, V. E. Sanders, W. Schleich, and M. O. Scully, *Rev. Mod. Phys.* **57**, 61 (1985).
- [2] F. Aronowitz, in *Laser Applications*, edited by M. Ross (Academic Press, New York, 1971), Vol. 1, pp. 133–200.
- [3] H. C. Lefèvre, *The Fiber-Optic Gyroscope* (Norwood, MA, Artech House, 1993).
- [4] F. Dell’Olio, T. Tatoli, C. Ciminelli, and M. Armenise, *J. Europ. Opt. Soc. Rap. Public.* **9**, 14013 (2014).
- [5] M. Terrel, M. J. F. Dignonnet, and S. Fan, *Laser Photon. Rev.* **3**, 452 (2009).
- [6] S. Sunada and T. Harayama, *Opt. Express* **15**, 16245 (2007).
- [7] R. Sarma, L. Ge, and H. Cao, *J. Opt. Soc. Am. B* **32**, 1736 (2015).
- [8] L. Ge, R. Sarma, and H. Cao, *Optica* **2**, 323 (2015).
- [9] J. Scheuer, *Opt. Express* **15**, 15053 (2007).
- [10] B. Z. Steinberg, *Phys. Rev. E* **71**, 056621 (2005).
- [11] W. Liang, V. S. Ilchenko, A. A. Savchenkov, E. Dale, D. Eliyahu, A. B. Matsko, and L. Maleki, *Optica* **4**, 114 (2017).
- [12] K. Suzuki, K. Takiguchi, and K. Hotate, *J. Lightwave Technol.* **18**, 66 (2000).
- [13] H. Mao, H. Ma, and Z. Jin, *Opt. Express* **19**, 4632 (2011).
- [14] P. J. R. Laybourn, M. Sorel, G. Giuliani, and S. Donati, *Proc. SPIE* **3620**, 322 (1999).
- [15] M. N. Armenise, V. M. N. Passaro, F. Leonardis, and M. Armenise, *J. Lightwave Technol.* **19**, 1476 (2001).
- [16] T. Zhang, G. Qian, Y.-Y. Wang, X.-J. Xue, F. Shan, R.-Z. Li, J.-Y. Wu, and X.-Y. Zhang, *Sci. Rep.* **4**, 3855 (2014).
- [17] H. Zhang, J. Liu, J. Lin, W. Li, X. Xue, A. Huang, and Z. Xiao, *Appl. Phys. A* **122**, 501 (2016).
- [18] E. J. Post, *Rev. Mod. Phys.* **39**, 475 (1967).
- [19] M. S. Shahriar, G. S. Pati, R. Tripathi, V. Gopal, M. Messall, and K. Salit, *Phys. Rev. A* **75**, 053807 (2007).
- [20] H. N. Yum, M. Salit, J. Yablon, K. Salit, Y. Wang, and M. S. Shahriar, *Opt. Express* **18**, 17658 (2010).
- [21] M. A. Terrel, M. J. F. Dignonnet, and S. Fan, *Proc. SPIE* **7612**, 76120B (2010).
- [22] M. Salit, K. Salit, and P. E. Bauhahn, *Proc. SPIE* **8273**, 82730H (2012).
- [23] T. Qu, K. Yang, X. Han, S. Wu, Y. Huang, and H. Luo, *Sci. Rep.* **4**, 7098 (2014).
- [24] D. D. Smith, H. A. Luckay, H. Chang, and K. Myneni, *Phys. Rev. A* **94**, 023828 (2016).
- [25] S. Schwartz, F. Goldfarb, and F. Bretenaker, *Opt. Eng.* **53**, 102706 (2014).
- [26] Z. Wang and B. Yuan, *Sci. Rep.* **5**, 12026 (2015).
- [27] J. Wiersig, *Phys. Rev. Lett.* **112**, 203901 (2014); *Phys. Rev. A* **93**, 033809 (2016).
- [28] N. Zhang, S. Liu, K. Wang, Z. Gu, M. Li, N. Yi, S. Xiao, and Q. Song, *Sci. Rep.* **5**, 11912 (2015).
- [29] A. Hassan, H. Hodaei, W. Hayenga, M. Khajavikhan, and D. Christodoulides, in *Advanced Photonics 2015*, OSA Technical Digest (online) (Optical Society of America, Washington, DC, 2015), paper SeT4C.3, doi:10.1364/SENSORS.2015.SeT4C.3.
- [30] Z.-P. Liu, J. Zhang, S. K. Ozdemir, B. Peng, H. Jing, X.-Y. Lü, C.-W. Li, L. Yang, F. Nori, and Y.-X. Liu, *Phys. Rev. Lett.* **117**, 110802 (2016).
- [31] J. Ren, H. Hodaei, G. Harari, A. U. Hassan, W. Chow, M. Soltani, D. N. Christodoulides, and M. Khajavikhan, *Opt. Lett.* **42**, 1556 (2017).
- [32] T. Kato, *Perturbation Theory for Linear Operators* (Springer, New York, 1966).
- [33] M. V. Berry, *Czech. J. Phys.* **54**, 1039 (2004).
- [34] W. D. Heiss, *J. Phys. A* **45**, 444016 (2012).
- [35] C. Dembowski, H.-D. Graf, H. L. Harney, A. Heine, W. D. Heiss, H. Rehfeld, and A. Richter, *Phys. Rev. Lett.* **86**, 787 (2001).
- [36] S.-B. Lee, J. Yang, S. Moon, S.-Y. Lee, J.-B. Shim, S. W. Kim, J.-H. Lee, and K. An, *Phys. Rev. Lett.* **103**, 134101 (2009).
- [37] B. Zhen, C. W. Hsu, Y. Igarashi, L. Lu, I. Kaminer, A. Pick, S.-L. Chua, J. D. Joannopoulos, and M. Soljačić, *Nature* **525**, 354 (2015).
- [38] M. Liertzer, Li Ge, A. Cerjan, A. D. Stone, H. E. Türeci, and S. Rotter, *Phys. Rev. Lett.* **108**, 173901 (2012).
- [39] L. Feng, Z. J. Wong, R.-M. Ma, Y. Wang, and X. Zhang, *Science* **346**, 972 (2014).
- [40] H. Hodaei, M.-A. Miri, M. Heinrich, D. N. Christodoulides, and M. Khajavikhan, *Science* **346**, 975 (2014).
- [41] K.-H. Kim, M.-S. Hwang, H.-R. Kim, J.-H. Choi, Y.-S. No, and H.-G. Park, *Nat. Commun.* **7**, 13893 (2016).
- [42] S. Richter, T. Michalsky, C. Sturm, B. Rosenow, M. Grundmann, and R. Schmidt-Grund, *Phys. Rev. A* **95**, 023836 (2017).
- [43] A. P. Seyranian and A. A. Mailybaev, *Multiparameter Stability Theory with Mechanical Applications* (Singapore, World Scientific, 2003).

- [44] A. P. Seyranian, O. N. Kirillov, and A. A. Mailybaev, *J. Phys. A* **38**, 1723 (2005).
- [45] G. Demange and E.-M. Graefe, *J. Phys. A* **45**, 025303 (2012).
- [46] A. Luongo, *J. Sound Vib.* **185**, 377 (1995).
- [47] K. Hashimoto, K. Kanki, H. Hayakawa, and T. Petrosky, *Prog. Theor. Exp. Phys.* **2015**, 023A02 (2015).
- [48] R. Sarma, L. Ge, J. Wiersig, and H. Cao, *Phys. Rev. Lett.* **114**, 053903 (2015).
- [49] R. J. C. Spreeuw, R. C. Neelen, N. J. van Druten, E. R. Eliel, and J. P. Woerdman, *Phys. Rev. A* **42**, 4315 (1990).
- [50] S. Sunada, S. Tamura, K. Inagaki, and T. Harayama, *Phys. Rev. A* **78**, 053822 (2008).
- [51] H. J. Arditty and H. C. Lefèvre, *Opt. Lett.* **6**, 401 (1981).
- [52] S. Sunada and T. Harayama, *Phys. Rev. A* **74**, 021801(R) (2006).
- [53] D. Goldring, U. Levy, and D. Mendlovic, *Opt. Express* **15**, 3156 (2007).
- [54] A. Pick, B. Zhen, O. D. Miller, C. W. Hsu, F. Hernandez, A. W. Rodriguez, M. Soljačić, and S. G. Johnson, *Opt. Express* **25**, 12325 (2017).
- [55] S. Ezekiel and S. R. Balsamo, *Appl. Phys. Lett.* **30**, 478 (1977).
- [56] J. Zhu, S. K. Özdemir, L. He, and L. Yang, *Opt. Express* **18**, 23535 (2010).
- [57] B. Peng, S. K. Özdemir, M. Liertzer, W. Chen, J. Kramer, H. Yilmaz, J. Wiersig, S. Rotter, and L. Yang, *Proc. Natl. Acad. Sci. USA* **113**, 6845 (2016).